Research Article

Research on the impact of ship traffic flow on the restricted channel segment of the middle Yangtze River based on traffic wave theory

Ting Liu[1] · Gabriel Lodewijks[2]

Received: 23 February 2021 / Accepted: 7 July 2021
Published online: 22 July 2021

Abstract

Abstract On the basis of the influence of dry season on ship traffic flow, the gathering and dissipating process of ship traffic flow was researched with Greenshields linear flow—density relationship model, the intrinsic relationship between the ship traffic congestion state and traffic wave in the unclosed restricted channel segment was emphatically explored when the ship traffic flow in a tributary channel inflows, and the influence law of multiple traffic waves on the ship traffic flow characteristics in unclosed restricted segment is revealed. On this basis, the expressions of traffic wave speed and direction, dissipation time of queued ships and the number of ships affected were provided, and combined with Monte Carlo method, the ship traffic flow simulation model in the restricted channel segment was built. The simulation results show that in closed restricted channel segment the dissipation time of ships queued is mainly related to the ship traffic flow rate of segments A and C, and the total number of ships affected to the ship traffic flow rate of segment A. And in unclosed restricted channel segment, the dissipation time and the total number of ships affected are also determined by the meeting time of the traffic waves in addition to the ship traffic flow rate of segments. The research results can provide the theoretical support for further studying the ship traffic flow in unclosed restricted channel segment with multiple tributaries

Article Highlights

1. The inflow of tributaries' ship traffic flows has an obvious impact on the traffic conditions in the unenclosed restrictedchannel segment.
2. The interaction and influence between multiple ship traffic waves and the mechanism of generating new traffic waves areexplained.
3. The expression of both dissipation time of queued ships and the total number of ships affected in the closed and unclosedrestricted channel segment are given.

Keywords Ship traffic flow · Restricted channel segment · Wavefront · Wave speed · Gathering wave · Dissipating wave

JEL R41 · L91

✉ Ting Liu, cream4.24@163.com; Gabriel Lodewijks, g.lodewijks@unsw.edu.au | [1]Jiujiang University, Jiujiang 332005, China. [2]The University of New South Wales, Sydney, NSW 2052, Australia.

1 Introduction

The middle reaches of the Yangtze River, as the throat segment of the golden waterway of the Yangtze River, are characterized by curved channels, numerous shallow shoals, different river types and river bed boundary conditions along the reach, and complicated and changeable navigation environment. Changes in precipitation and temperature caused by climate change will directly or indirectly lead to the changes in river water level, erosion and deposition characteristics, and river morphology, resulting in continuous high or low water level. For example, in the spring of 2007, the middle reaches of the Yangtze River encountered exceptionally low water level in a century, and in July 2012, due to the extreme flood peak of the Yangtze River, the Three Gorges ship lock was suspended and the navigation in some channel segments of the middle Yangtze River was restricted or banned, and thousands of ships were stranded. From 2012 to 2019, the extreme low water level of the middle Yangtze River continued to occur, and in November 2019, the water level in the middle reaches of the Yangtze River reached its lowest record in 116 years. This change in the frequency and duration of extreme hydrological events will have a serious impact on navigation along the Yangtze River.

In the dry season, the channel is further narrowed, which will increase the risk of ships encounter, and ships are easy to get touching the shore and grounding. Shallow water effect will occur because of low water level, resulting in the decline of ship speed and rudder force, the increase of ship control difficulty, traffic jams and even congestion. During the flood period, the scouring force of the water stream becomes smaller, silt and sand are deposited in the channel, and the water level of the channel gradually decreases. The cargo ship with deep draft is likely to be stranded. The frequent occurrence of extreme hydrologic events has a great negative impact on the shipping organization, transportation safety and transportation economy of the Yangtze River.

From the successful experience of foreign basin development, the industrial agglomeration and central position of the countries or regions along the river basin have largely benefited from the improvement of the channel conditions and shipping methods. At present, under the background of China's strategic implementation of the Yangtze River Economic Belt, the research on ship traffic flow and navigation efficiency in the middle reaches of the Yangtze River has become a hot spot. Some scholars focused on the theoretical research of traffic flow. Wang, Ren and Wu studied the relationship among traffic flow rate, density and speed, and simulated traffic flow with related theories of fluid mechanics [1–3]. Another part of scholars concentrated on the research of ship traffic flow of inland waterway, divided into the following directions.

The first was to study the characteristics of ship traffic flow in inland waterway. Liu and Lu et al. [4, 5] studied the closure measures of navigation adopted in the channel under the extreme water level, and explained the process of gathering and dissipating process of ship traffic flow after the closure of navigation using the traffic wave theory. Liu et al. and Liao [6, 7] respectively analyzed the characteristics of ship traffic flow in sea and inland waterway. In order to improve the safety of Marseille Port, Elloumi et al. [8] developed the decision support system to conduct the statistical analysis on the behavior characteristics of medium and small ships in the port. In 2013, Martin et al. [9] drew the diagram of the relationship between "flow-speed", "speed-density" and "speed-flow" according to the vehicle traffic flow rate in Frankfurt, Germany. Kujala studied the distribution of basic characteristic elements such as vessel flow; composition and position in the ship lock waters [10]. Liu investigated the characteristics, influencing factors and evolution mechanism and model of ships under complex navigable conditions [11].

The second was to study the passing capacity or efficiency of inland waterway. Dong et al. [12] studied the passing ability of natural and channelized channels. Based on integrating ship traffic flow theory and the relative analytical formula, Zhang et al. [13] established the calculation method of passing capability under any ship type. Yang et al. [14] proposed some representational parameters of ship traffic congestion status in restricted channel segment, and discussed the internal correlation between ship traffic congestion status and character of ship motion by using Monte Carlo simulation.

The third is the use of Greenshields model in macro-transportation planning. Since the Greenshields model is simple in form and convenient for the derivation and analysis of theoretical formulas, although it has some shortcomings in its application, it is still widely used in the study of road traffic flow and is a very important model [15–19]. The relationship of velocity-density in ship traffic flow is similar to that in road traffic flow, but the influence factors of the former has some difference from the latter. Ship traffic flow is not only affected by the larger volume, lower speed, larger spacing and smaller density of ships, but also by the speed of water flow, and the regulations that generally in a single channel ships are not allowed to exceed. Therefore, the velocity-density model should be selected in the study of ship traffic flow, which is relatively simple in form and can basically guarantee the accuracy of macroscopic analysis. At present, many scholars have explored the application of the Greenshields model in the study of the ship traffic flow of a single waterway, especially in the Yangtze River waterway, and major relevant literatures have been reported and some research results obtained. Such as Zhang et al. [20] he analyzed the inland ship traffic flow organizational characteristics with Greenshields speed—density linear relationship; Lu et al. [4] studied that impact of extreme water levels on characteristics of ship traffic flow in the middle reaches of Yangtze river using Greenshields model; Bai et al. and Zeng [21, 22] applied Greenshields model in the investigation of traffic efficiency based on traffic wave theory.

The fourth, various methods were used to conduct simulation research on ship traffic flow of inland waterway, but the research objects were mostly the ship traffic flow of inland waterway under long-term and normal water level [23–26]. By studying the characteristics of the bridge waters, Zhou analyzed the statistical information of ship attributes with statistical methods, mainly including the fitting of the distribution rules of the length, speed and spacing of ships, and performed the simulation analysis of ship traffic flow track [27]. In 2017, Wang et al. [28] established the complex simulation model of ship traffic flow considering influencing factors such as ship entry and departure rules, navigation rules and anchorage scale, to simulate ship navigation operation system, and to study the influencing factors of passing ability of channel. Asperen carried out the simulation study on ship arrival rules [29]. Based on historical data, Ercan studied the ship traffic behavior under different circumstances in the Istanbul Strait area, as well as the arrival time and waiting time of various types of ships, and established the traffic simulation model in the Istanbul Strait [30]. Kawamura et al. [31] studied ship behavior under severe sea conditions with simulation method. Qi et al. [32] analyzed the complex traffic phenomena of ships. Based on the spatial logic mapping (SLM) model, they proposed the process to solve the spatial discrete waterway rules and ship movement update rules, and established the ship traffic flow model based on cellular automata (CA). Qi et al. proposed a new maritime traffic model based on cellular automata with the characteristics of ship speed variation. The performance of the model was tested under weather and ocean conditions in the Dover Strait, the Changshan Channel and the Qiongzhou Strait [33]. Feng studied the situation of ship diversion or accident under partially closed channel, established the cellular automata model, and analyzed the influence of these conditions on the passing capacity of channel with numerical calculation method [34].

Due to the wide application of ship traffic flow and the great diversity of research objects, most of the literature selectively studies one or more ship traffic flow characteristics, such as the composition, behavior and arrival rules of the ship traffic flow, according to the application requirements. But there is little research on the impact of extreme water level changes on ship traffic flow of inland waterway. This research can enrich the research system of inland ship traffic flow to a certain extent, and provide the reference for Maritime Department in making the navigation plan and improving navigation efficiency, and further research the ship transport organization mode, ship type, port construction, and control mode to reduce the impact of extreme hydrological events in the middle reaches of Yangtze River, enhance the competitiveness of shipping, and develop the Yangtze River Economic Belt. Therefore, the research has certain theoretical significance and practical application value.

In this paper, under extreme water level, the ship traffic flow characteristics were analyzed with traffic wave theory, flow conservation law and Greenshields model. The gathering and dissipating process of ship traffic flow in closed and unclosed restricted channel segments were studied, the impact of the inflow of ship traffic flow in a tributary channel on the ship traffic flow in the unclosed restricted channel segment were discussed, and the relevant mathematical models of the ship traffic flow in the restricted channel segment were established. And the traffic flow characteristics of both closed and unclosed restricted channel segments were studied by using Monte Carlo method.

The contributions of the paper are as follows:

(1) The expressions of traffic wave speed and direction, the dissipation time and the total number of affected ships were given.
(2) The dissipation time of the queued ship is mainly related to the ship traffic flow rate of relative segments (upstream, downstream and tributary channel segment). Both total numbers of affected ships in closed and unclosed restricted segments are high-positive correlation with the ship traffic flow of the upstream segment.
(3) The interaction and influence laws among multiple traffic waves were given.

The research results can provide theoretical support for the in-depth study on the ship traffic flow in the unclosed restricted segment of the middle reaches of the Yangtze River.

2 The influence of dry season on the characteristics of ship traffic flow

The characteristics of ship traffic flow can be divided into macroscopic and microscopic categories. Macroscopic characteristics of ship traffic flow refer to the overall characteristics of continuously moving ships in a certain environment, waterway and time periods, which mainly include ship traffic flow rate, composition of ship traffic flow, and law of ship arrival and distribution of waiting time. Microscopic characteristics refer to the characteristics related to the position, direction, speed and ship domain of a single ship.

The dry season in the middle Yangtze River is generally from December to March of the following year, because of the low water level and slow water flow, shoals will appear in some channel segments (in the following text, the channel segments are referred to as segments.), so these segments are often curved, and make ship operation more difficult, passing capacity of these segments declined, and ship density relatively increased. At the peak of ship traffic flow, in order to guarantee ship's safe navigation, Maritime Department will take some measures such as reducing ship loading rate, one-way passing in different time periods, diverting cargoes by other transportation modes, and even closuring channel and so on. The changes of characteristics of ship traffic flow are as follows:

2.1 Ship traffic flow rate

In the dry season, the traffic conditions in some channels become worse so that the passing capacity of channels is reduced, and ship congested, which leads to the reduction or uneven distribution of ship traffic flow.

2.2 Ship composition

In the dry season, because the water depth cannot meet the ship's full draft, the ship may need to reduce its cargoes, and the proportion of smaller tonnage ships in the ship traffic flow may increase.

2.3 Law of ship arrival

Under normal circumstances, the law of ship arrival usually follows Poisson's distribution or Normal distribution. In the dry season, some ships need to wait for the tide to enter the port, and the law of ship arrival changed, which may be achieved by the intermittent traffic flow instead of the steady traffic flow. The equilibrium between busy time and idle time in the port is broken, and the imbalance state is intensified.

2.4 Distribution of waiting time

When larger ship traffic flow, poor channel conditions, channel congestion, retention or security risks occur, Maritime Department may control the ships passing through the channel segment according to the actual channel conditions, such as traffic or time restriction, etc. to shunt ships, and even to ban navigation in severe case, which can cause additional time-consuming. In addition, the low water level will also cause the work efficiency of loading and unloading equipment of the port berth to be decreased, so that the waiting time of ships is increased.

2.5 Ship speed

The ship's sailing speed is determined by calm water speed of ship and water flow velocity of channel. In the dry season, the water level and the water speed all decreases. At this time, the Maritime Department sometimes requires reducing the ship's cargoes. The decrease of ship load and the influence of water flow velocity of channel will lead to the change of ship speed, which will affect the distribution of the ship speed.

3 Ship traffic flow model

3.1 Ship traffic flow theory

Assume that there are two adjacent segments *A* and *B* (without other entrances between the two ends) with different density and average speed of ship traffic flow, both density and average speed are ρ_A, v_A and ρ_B, v_B respectively, and the direction of ship speed is that of ship traffic flow. When ship traffic flow from segment *A* inflows into segment *B* and $\rho_A < \rho_B$, the ship traffic flow status changes. Ships line up one after another and gather into high-density queues, causing turbulence, congestion and even blockage; when $\rho_A > \rho_B$, the queued ships will start to evacuate into a queue with appropriate density. The vertical line *S* is used to divide two ship traffic flows of different densities, called wavefront *S*. The movement of the wavefront *S* in the ship traffic flow is called traffic wave [1, 2]; the speed of the wavefront *S* moving along the channel is called the wavefront speed, which is the absolute speed relative to the channel, referred to as traffic wave speed v_w. It also stipulates that the traffic wave speed is positive when the direction of the ship's traffic flow is the same, as shown in Fig. 1.

3.1.1 Basic mathematical model of ship traffic flow

Assuming that the same ship type is single, the ship speed is uniform, the ship heading is the same, and the channel width is unchanged, the basic equation of ship traffic flow rate can be expressed as:

$$q = \rho v \tag{1}$$

where *q* is ship traffic flow rate, that is the number of ships passing through a certain cross section per unit time,

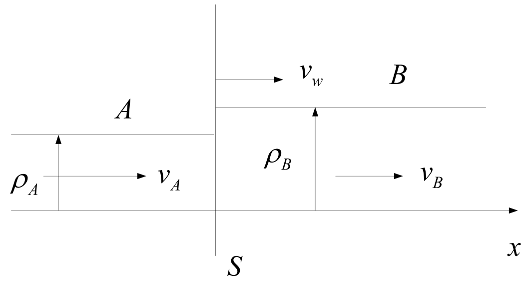

Fig. 1 Ship traffic flow status of two different densities

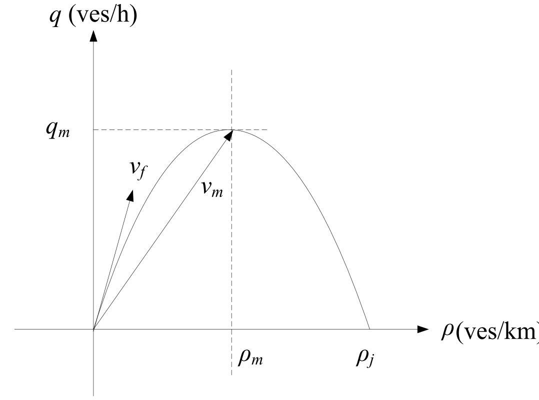

Fig. 2 The relationship between traffic flow rate and density

ves/h; ρ is the density of ship traffic flow, that is the number of ships in per unit length of channel segment, ves/km; and v is average speed of ship traffic flow, km/h.

3.1.2 Flow conservation law

According to mass conservation law in fluid mechanics, the number of ships leaving segment A per unit time t is equal to the number entering segment B.

$$\rho_A(v_A - v_w)t = \rho_B(v_B - v_w)t \tag{2}$$

where v_w is traffic wave speed, km/h; v_A–v_w is the speed of ship traffic flow relative to wavefront S before it enters wavefront S, km/h; v_B–v_w is the speed of ship traffic flow relative to wavefront S after it enters wavefront S, km/h.

So,

$$v_w = \frac{\rho_A v_A - \rho_B v_B}{\rho_A - \rho_B} \tag{3}$$

Substituting Eqs. (1) into (3), traffic wave speed can be expressed as:

$$v_w = \frac{q_A - q_B}{\rho_A - \rho_B} \tag{4}$$

3.1.3 Greenshields linear model

According to the linear speed-density relationship model proposed by Greensheilds, the average speed of ship traffic flow in segment i can be expressed as:

$$v_1 = v_f\left(1 - {}^{\rho_i}/_{\rho_j}\right) \tag{5}$$

Then the ship traffic flow rate in segment i is written as:

$$q_i = \left(1 - \frac{\rho_i}{\rho_j}\right)v_f\,\rho_i \tag{6}$$

where v_f is ship's free flow speed, km/h; ρ_j is congestion density, that is the density of ship traffic flow when traffic jams occur and the ship is almost impossible to navigate, ves/km.

The relationship between traffic flow rate and density is a quadratic function as shown in Fig. 2:

In Fig. 2, ship traffic flow rate increases with increasing density. When the density reaches ρ_m, ship traffic flow rate reaches the maximum flow rate q_m, the density at this time is the optimum density ρ_m, and the best speed is v_m; when density continues to increase, the flow rate begins to fall, when the ship traffic flow rate arrives blocking density ρ_j, ships are almost impossible to navigate, both speed and flow rate is zero. Take the derivative of Eq. (6) and set it equal to zero. And the following formula can be obtained:$\rho_m = \frac{1}{2}\rho_j$; $v_m = \frac{1}{2}v_f$. The maximum traffic flow rate can be expressed as:

$$q_m = \frac{1}{4}v_f\rho_j \tag{7}$$

3.2 Influence of traffic waves on ship traffic flow

Traffic wave describes the transformation process of two traffic flow states, as well as both direction and speed of transformation. When ship traffic flow enters segment B from segment A, and $\rho_A > \rho_B$, it indicates that the density decreases, the ship speed is up, and the generated traffic wave is called dissipating wave; when $\rho_A < \rho_B$, the density increases, the ship speed is down, and the traffic wave is gathering wave, the speed of traffic wave is represented by v_w.

3.2.1 $v_w > 0$

When $v_w > 0$, the traffic wave propagates downstream (i.e. forward propagation), consistent with the direction of the ship navigation. The traffic conditions of segment *B* will not affect the upstream segment *A*.

(1) When $q_A > q_B$ and $\rho_A > \rho_B$, the ships from the high-flow rate, high-density, low-speed segment *A* enter the low-flow rate, low-density, high-speed segment *B*, the traffic conditions become better. Due to the forward propagation of the traffic wave, the dense ship traffic flow of segment *A* begins to dissipate after entering segment *B*, forming a dissipating wave, but it will not improve the traffic conditions of upstream segment *A*, as shown in Fig. 3a.

There are two situations. One is when $\rho_A > \rho_m > \rho_B$, the ship density in segment *A* is greater than the optimum density and the segment is crowded. In order to ensure safety, the ship speed slows down and the ship traffic flow rate passing through is small. When the ship enters from segment *A* to segment *B*, the traffic conditions become better, the ship speed accelerates and the dense ship traffic flow begins to dissipate; the other is when $\rho_m > \rho_{A'} > \rho_B$, the segment *A* and *B* are not congestion. However, the traffic conditions of segment *B* are better than that of segment *A*, and the ships speed up after entering from segment *A* to segment *B*. But, they all fail to reach the optimum density and traffic flow rate.

(2) When $q_A < q_B$ and $\rho_A < \rho_B$, the ships from low-flow rate, low-density, high-speed segment *A* enter high-flow, high-density, low-speed segment *B*, traffic conditions become worse. Due to the forward propagation of the traffic wave, the ship traffic flow entering the segment *B* follows the original ship traffic flow of segment *B*, ship density increases so that gathering wave is formed, but it will not worsen the traffic conditions of upstream segment *A*, as shown in Fig. 3b.

There are two situations. One is $\rho_A < \rho_m < \rho_B$, the ship density in segment *B* is larger than the optimum density, and the segment is crowded, the ship speed is slow, and the ship traffic flow rate is low; the other is when $\rho_A < \rho_{B'} < \rho_m$, segment *A* and *B* are not congestion. However, the

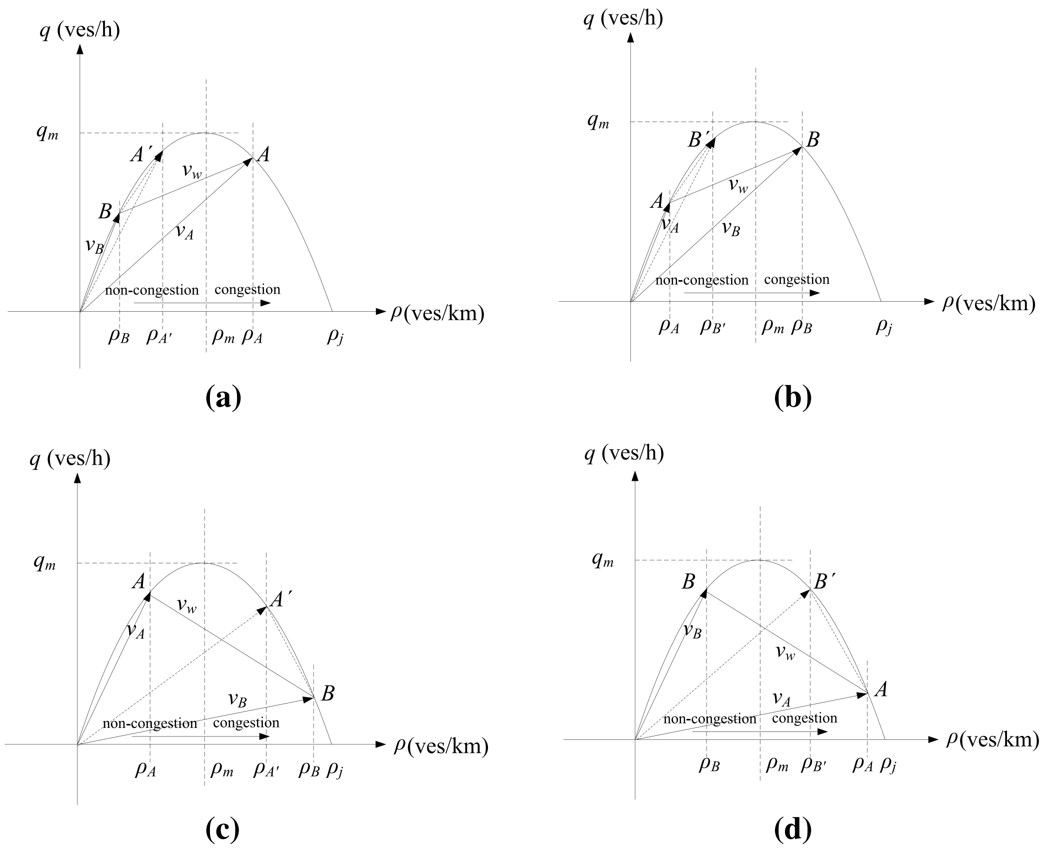

Fig. 3 The relationship between traffic flow rate and density in different cases. **a** The first case when $v_w > 0$. **b** The second case when $v_w > 0$. **c** The first case when $v_w < 0$. **d** The first case when $v_w < 0$

traffic conditions of segment *B* are worse than that of segment *A*, and the ship speed slows down after entering from segment *A* to segment *B*, but it does not reach the optimum density and traffic flow rate.

3.2.2 $v_w < 0$

When $v_w < 0$, the traffic wave propagates upstream (i.e. backward propagation), opposite to the direction of the ship speed. The upstream segment *A* is affected by the traffic condition of channel segment *B*.

(1) When $q_A > q_B$ and $\rho_A < \rho_B$, the ships from high-flow rate, low-density, high-speed segment *A* enter low-flow rate, high-density, low-speed segment *B*, the gathering wave is formed. Among them, when $\rho_A < \rho_m < \rho_B$, segment *B* has been congested, the traffic conditions of upstream segment *A* is affected by the obstruction of segment *B*, the ships slow down and begin to queue into segment *B*. When $\rho_m < \rho_{A'} < \rho_B$, both segments *A* and *B* have been congestion, the traffic conditions of segment *B* is worse, and the traffic conditions of upstream segment *A* will also deteriorate further, the queue is longer and more congestion. Both cases are shown in Fig. 3c.
(2) When $q_A < q_B$ and $\rho_A > \rho_B$, the ships from the low-flow rate, high-density, low-speed segment *A* enter the high-flow rate, low-density, high-speed segment *B*, dissipating wave is formed. Among them, when $\rho_A > \rho_m > \rho_B$, the traffic conditions of downstream segment *B* is favorable, the ship traffic flow can be accelerated into segment *B*, the congestion of segment *A* can be alleviated. When $\rho_A > \rho_{B'} > \rho_m$, although both segments *A* and *B* are congestion, the traffic conditions of segment *B* is better than that of segment *A*, which can improve the traffic conditions of upstream segment *A*, and the queue condition of segment *A* is dissipated, as shown in Fig. 3d.

3.2.3 $v_w = 0$

When $v_w = 0$, only $q_A = q_B$, this is a change in the state of the traffic flow of two ships with the same flow but different speeds and densities. The traffic wave does not move and does not have any impact on upstream and downstream. According to the above analysis, when the ship traffic flow changes from low density to high density, gathering wave will be formed, and when the ship traffic flow changes from high density to low density, dissipating wave will be formed. Traffic wave has a great impact on the existing traffic conditions, which should be the focus of the study.

4 Analysis of ship traffic flow characteristics in restricted channel segment

4.1 Analysis of ship traffic flow characteristics in closed restricted channel segment

In the dry season, the water level is low and the flow speed is declined, so that some segments are shallow and narrow. As a result, navigation bottlenecks are created, and the passing capacity of the segment is restricted, the density of ships in the segment is relatively increased and the ship speed is declined. The closed segment means that there are no other tributaries on the main channel, and the ship traffic flow rate mainly comes from upstream segment.

Related assumptions are as follows.

(1) Assuming that segments *A* to *C* are closed, the width of the segments is the same, and there are no other tributaries, that is, all ship traffic flow rate flowing into segment *A* will eventually flow out of segment *C*.
(2) In the dry season, segment *B* becomes a restricted one due to the deterioration of navigation conditions in the channel, and its maximum passing capacity q_{Bm} is less than that of segments *A* and *C*, that is $q_{Bm} < q_{Am} = q_{Cm}$, at this time, the restricted segment *B* reaches the maximum passing capacity, that is $q_B = q_{Bm}$ and $\rho_B = \rho_m$.
(3) In order to ensure safety and reduce congestion of the channel, the Maritime Department usually adopts the control measures of one-way release at different times during peak periods; ship overtaking is prohibited within restricted segment. When the ship of segment *A* enters segment *B*, the ship needs to slow down. When the ship leaves segment *B* and reaches the downstream segment *C*, the ship starts to accelerate, as shown in Fig. 4.

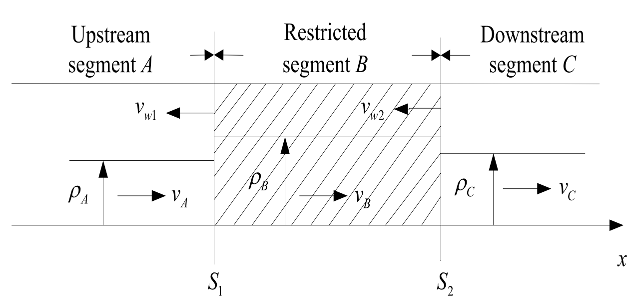

Fig. 4 The closed restricted segment

4.1.1 *Wavefront S_1*

When the ship traffic flow from the low-density segment *A* enters the high-density segment *B*, that is, $\rho_A < \rho_B$ (according to the analysis in Chapter 3, the gathering wave is generated this moment), wavefront S_1 is generated, and the wave speed is v_{w1}. Ship traffic flow can be smooth sailing in segment *A*, but due to the limited passing capacity of segment *B*, the density of ships in the segment *B* is high and the ship speed is slow. At this time, segment *B* has reached the maximum passing capacity, that is $v_A > v_B$ and $\rho_A < \rho_B = \rho_m$. There are two situations here. One is when $q_A > q_B$, $v_{w1} < 0$; it indicates that the traffic wave propagates to upstream segment *A*, and the direction of the traffic wave is opposite to that of ship navigation. Therefore, the traffic conditions of upstream segment *A* are affected, and the ships need to slow down and queue to enter the restricted segment *B*. The ships start to queue at wavefront S_1, and the queue propagates to upstream segment *A*, so gathering wave is generated. The other is when $q_A < q_B$, so $v_{w1} > 0$; it indicates that the traffic wave propagates to downstream segment *B*, and the direction of the traffic wave is consistent with that of the ship navigation. The ship traffic flow of segment *A* enters segment *B*, due to the increase in density, the ships will slow down and queue up at the back of the ship traffic flow in the original segment *B*, forming gathering wave, but will not affect the traffic conditions of upstream segment *A*, as shown in Fig. 5.

4.1.2 *Wavefront S_2*

When the ship traffic flow leaves the high-density segment *B* and enters the low-density segment *C*, that is, $\rho_B > \rho_C$ (according to the analysis in Chapter 3, the dissipating wave is generated this moment), wavefront S_2 is generated, and the wave speed is v_{w2}. Because the traffic condition of downstream segment *C* is good, that is, $v_B < v_C$ and $\rho_B = \rho_m > \rho_C$. There are two situations here. One is when $q_B > q_C$, so $v_{w2} > 0$; it indicates that the traffic wave propagates to downstream segment *C*, and the direction of the traffic wave is consistent with to that of ship navigation. So the dissipating wave is formed in channel segment *C*, but it will not affect the upstream traffic conditions. Second, when $q_B < q_C$, then $v_{w2} < 0$; it indicates that the traffic wave propagates to upstream segment *B*, and the direction of the traffic wave is opposite to that of the ship navigation. The dissipating wave propagates upstream, the existing queues begin to dissipate, and the traffic conditions of upstream segment *B* are improved.

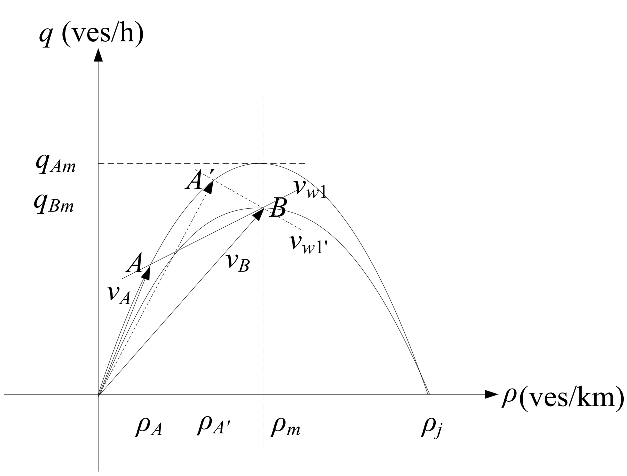

Fig. 5 The relationship between traffic flow rate and density of the closed restricted segment

4.1.3 Analysis of gathering and dissipating waves

There are two situations in the gathering wave and the dissipating wave. One is that the gathering wave and the dissipating wave will never meet, and the other is that that the gathering wave and the dissipating wave will meet.

(1) The gathering wave and the dissipating wave will never meet

There are two situations: One is when $v_{w2} > 0$, no matter if $v_{w1} > 0$ or $v_{w1} < 0$, the gathering wave and the dissipating wave will not meet, that is, the queuing situation always exists in this case. The other is when $v_{w2} > 0$, $v_{w1} < 0$ and $|v_{w2}| < |v_{w1}|$, the queuing speed of ships is greater than the dissipating speed, and the queuing will continue to increase until the off-peak period, when the traffic flow rate decreases, the queue slowly dissipates on its own. These two situations are not discussed in this paper.

(2) The gathering wave and the dissipating wave will meet

There are two situations. One is when $v_{w2} < 0$, $v_{w1} < 0$ and $|v_{w2}| > |v_{w1}|$; the other is when $v_{w2} < 0$ and $v_{w1} > 0$, both the gathering wave and the dissipating wave will meet, which is the focus of this paper.

According to as shown in Fig. 4, in the peak period the Maritime Department uses control measures of one-way release at different time. The ship overtaking is prohibited in the restricted segment *B*; when $\rho_A < \rho_B$, the ships in segment *A* need to slow down entering into the segment *B*, and line up behind the ship traffic flow of the original segment *B* at wave speed v_{w1}, so the density of the queue is ρ_B, which generates gathering wave. When $\rho_B > \rho_C$, the ship that leaves segment *B* and reaches downstream segment *C* begins to accelerate, and dissipate the queue at wave speed v_{w2}, which generates dissipating wave. According to Eq. (3), the wave speed v_{w1} and v_{w2} can be expressed as:

$$v_{w1} = \frac{\rho_A v_A - \rho_B v_B}{\rho_A - \rho_B} \tag{8}$$

$$v_{w2} = \frac{\rho_B v_B - \rho_C v_C}{\rho_B - \rho_C} \tag{9}$$

The front end of the ship traffic flow in the restricted segment B is dissipated at the wave speed v_{w2}, and that of the back is still gathering at the wave speed v_{w1}. The dissipation time T is the time for the dissipating wave to catch up with the gathering wave. The moment, all queued ships are completely dispersed, so T can be expressed as:

$$T = L_B / \left| v_{w2} - v_{w1} \right| \tag{10}$$

Where T is dissipation time of the queue, h; L_B is the length of the restricted segment B, km.

The total numbers of ships affected by closed restricted segment N_B can be expressed as:

$$N_b = \rho_B \left| v_B - v_{w1} \right| T \tag{11}$$

4.2 Analysis of ship traffic flow characteristics in unclosed restricted segment

The unclosed segment refers to the main segment with tributaries Both inflow and outflow of ship traffic flows of tributaries make the distribution of ship traffic flow in the main segment changed. At this time, the ship traffic flow in the tributaries will directly affect the operation state of the ship traffic flow in the main segment. For the ship traffic flow inflowing from tributaries, it is limited by the passing capacity of the main segment; on the other hand, it has an interweaving influence on the ship traffic flow of the main segment due to the inflowing, which in turn limits its passing capacity.

Assumptions:

(1) Segment B is the restricted segment among segment A, B and C. Segment D is a tributary segment on segment B. When the upstream ship traffic flow reaches here, there will be the outflow and inflow of ship traffic flow. Segment D divides segment B into parts B_1 and B_2, as shown in Fig. 6.

(2) The ship traffic flow of segment D is steady; Δq_D is the difference between the ship traffic flow rates inflowed from segment D and outflowed from segment B. Both $\Delta q_D > 0$ and $\Delta q_D < 0$ represent the number of ships inflowing and outflowing of segment B respectively. Before the traffic flow rate Δq_D of segment D inflows or outflows segment B, the ship traffic flow rate of segment B (including B_1 and B_2) maintains the maximum traffic flow rate q_{Bm}.

(3) The ship traffic flow of channel segment D has the priority to inflow.

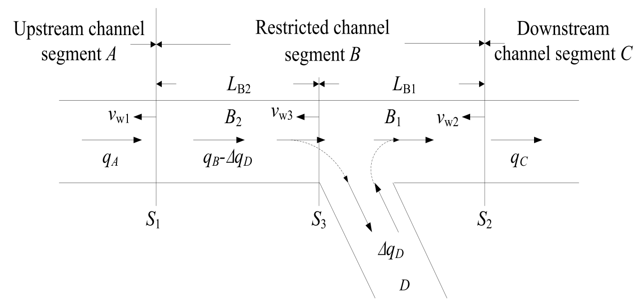

Fig. 6 The unclosed restricted segment

As can be seen from Fig. 6, when Δq_D outflows from segment B_2, that is, $\Delta q_D < 0$, the density of segment B_2 decreases and the traffic condition improves. When Δq_D inflows into segment B_1, namely $\Delta q_D > 0$, ship traffic flow rate in upstream segment B_2 allowed to enter segment B_1 is q_{Bm}—Δq_D, but at this time the ship traffic flow rate in segment B_2 is q_{Bm}, therefore the ships with Δq_D will be stuck, while the ships in segment A will continue to inflow. As a result, the density of segment B_2 rises, the channel congests and the traffic condition deteriorates. At the moment, the wavefront S_3 with wave speed v_{w3} is formed between channel segment B_1 and B_2, the wavefront S_1 with wave speed v_{w1} is formed between channel segment B_2 and A, and the wavefront S_2 with wave speed v_{w2} is formed between channel segment B_1 and C.

4.2.1 *Wavefront S_3*

Since segment B_2 has only ship traffic flow rate q_B–Δq_D that can be inflowed into segment B_1, which indicates that maximum passing capacity of segment B_2 has changed from the original largest passing capacity of restricted segment B ($q_{B_1m} = q_{B_2m} = q_{Bm}$) to q_B–Δq_D. Therefore, segment B_2 occurs congested, traffic flow density increases and speed decreases, it can be seen that segment B_2 becomes the bottleneck section in segment B. The ship traffic flow status changes from B_2 of the traffic flow rate-density curve to $B_2{}'$, that is, the maximum passing capacity of segment B_2 is equal to that of the original restricted segment B, which exceeds the maximum passing capacity. As a result, the density increases from ρ_m to $\rho_{B2'}$. Ship speed declines from v_{B2} to $v_{B2'}$, ship traffic flow rate drops to as q_{Bm}–Δq_D, namely $q_{B2'} = q_{B2m} = q_{Bm}$–$\Delta q_D$, as shown in Fig. 7.

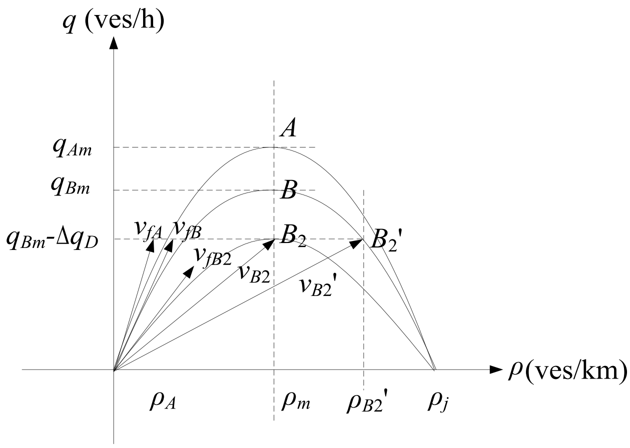

Fig. 7 The relationship between traffic flow rate and density of the unclosed restricted segment

According to Eq. (6), the maximum passing capacity of segment B_2 can be expressed as:

$$q_{Bm} - \Delta q_D = \left(1 - \frac{\rho_{B_2'}}{\rho_j}\right) v_{fB} \rho_{B_2'} \tag{12}$$

where, v_{fB} is the ship's free speed in the original segment B, km/h.

Then the traffic flow density $\rho_{B2'}$ of segment B_2 can be expressed as:

$$\rho_{B_2'} = \sqrt{\frac{\rho_j^{\,2}}{4} - \frac{\left(q_{Bm} - \Delta q_D\right)\rho_j}{v_{fB}}} + \frac{\rho_j}{2} \tag{13}$$

According to Eq. (7), the original free speed v_{fB} of ship in segment B, free speed v_{fB_2} of ship and traffic flow density $\rho_{B2'}$ in segment B_2 can be written as:

$v_{fB} = \frac{4q_{Bm}}{\rho_j}, v_{fB_2} = \frac{4(q_{Bm}-\Delta q_D)}{\rho_j}$,and

$$\rho_{B_2'} = \sqrt{\frac{\rho_j^{\,2}}{4} - \frac{\left(q_{Bm} - \Delta q_D\right)\rho_j^{\,2}}{4q_{Bm}}} + \frac{\rho_j}{2}$$

Since $\rho_m < \rho_{B2'}$, dissipating wave is generated, and the wave speed v_{w3} of wavefront S_3 can be expressed as:

$$v_{w3} = \frac{q_{Bm} - \left(q_{Bm} - \Delta q_D\right)}{\rho_{m-}\rho_{B_2'}} \tag{14}$$

Due to $\Delta q_D > 0$ and $\rho_m < \rho_{B2'}$, so $v_{w3} < 0$, the dissipating wave propagates from S_3 to upstream segment B_2.

4.2.2 *Wavefront S_1*

In unclosed restricted segment, the wave speed v_{w1} of wavefront S_1 will be different from the previous analysis of closed restricted segment, can be expressed as:

$$v_{w1} = \frac{q_A - \left(q_{Bm} - \Delta q_D\right)}{\rho_A - \rho_{B_2'}} \tag{15}$$

Since $\rho_A < \rho_{B2'}$, gathering wave is generated. There are two situations: (1) if $q_A > q_{Bm}$–-Δq_D, then $v_{w1} < 0$, the gathering wave propagates from S_1 to upstream segment A, and ships queue up in segment A with the density of $\rho_{B2'}$; (2) if $q_A < q_{Bm}$-Δq_D, then $v_{w1} > 0$, the gathering wave is propagates from S_1 to the downstream section B_2, and ships queue up in the section B_2 with the density of $\rho_{B2'}$.

4.2.3 *Wavefront S_2*

In unclosed restricted segment, the wave speed v_{w2} of wavefront S_2 is exactly the same as the analysis of the closed restricted segment, see the analysis in 4.1.2.

4.2.4 Analysis of gathering and dissipating waves

According to the above analysis, three wavefronts S_1, S_2 and S_3 will be formed in the unclosed restricted segment, and their wave speeds are v_{w1}, v_{w2} and v_{w3} respectively. The v_{w1} is the wave speed of the gathering wave, and v_{w2} and v_{w3} are the wave speed of the dissipating wave. When two traffic waves meet, a new traffic wave appears and sequentially propagates. According to the analysis of 4.1.3, the paper does not discuss the case of $v_{w2} > 0$. When $v_{w2} < 0$, there are two situations One is when v_{w2} and v_{w3} meet first (i.e. $|v_{w2}| > |v_{w3}|$, the meeting time is T_{23}) to produce a new dissipating wave that propagates to upstream at the wave speed v_{w4}. When the v_{w4} meets v_{w1}, queued ships are disappeared. The other is when v_{w3} and v_{w1} meet first (i.e. $|v_{w3}| > |v_{w1}|$, the meeting time is T_{31}), queued ships have all disappeared. Both T_{23} and T_{31} can be respectively expressed as:

$$T_{23} = L_{B_1} / \left| v_{w2} - v_{w3} \right| \tag{16}$$

$$T_{31} = L_{B_2}/|v_{w3} - v_{w1}| \quad (17)$$

(1) $T_{23} > T_{31}$

When $T_{23} > T_{31}$, it means that the gathering wave(wave speed is v_{w1}) and the dissipating wave (wave speed is v_{w3}) meet first, the front end of the ship traffic flow in the segment B_2 is dissipating at wave speed v_{w3}, and the back end is still gathering at wave speed v_{w1}. The dissipation time T is the encounter time of the dissipating wave and the gathering wave. At this time, all the queued ships due to the gathering wave are completely dissipated, and the dissipation time T can be expressed as:

$$T = T_{31} = L_{B_2}/|v_{w3} - v_{w1}| \quad (18)$$

The total numbers of ships affected by unclosed restricted segment N_B can be expressed as:

$$N_b = \rho_{B'2}|v_{B'2} - v_{w31}| = \rho_{B'2}\left|v_{B'2} - v_{w1}L_{B2}/|v_{w3} - v_{w1}|\right| \quad (19)$$

(2) $T_{23} < T_{31}$

When $T_{23} < T_{31}$, it means that two dissipating waves meet first, the wave speed is v_{w2} and v_{w3} respectively, and a new dissipating wave is generated at wave speed v_{w4}, which continues to propagate upstream. The dissipating wave speed v_{w4} is expressed as:

$$v_{w4} = \frac{q_C - q_{B'_2}}{\rho_C - \rho_{B'_2}} \quad (20)$$

When the new dissipating wave is generated at wave speed v_{w4}. The front end of the ship traffic flow in segment B_2 is dissipating at wave speed v_{w4}, while the back end is still gathering at wave speed v_{w1}. When the new dissipating wave speed v_{w4} and the gathering wave speed v_{w1} meet, at this time, all queued ships will dissipate. The dissipation time T is divided into two parts: one is the meeting time of two dissipating waves speed v_{w2} and v_{w3}, i.e. T_{23}; the other is the meeting time of dissipating wave v_{w4} and gathering wave v_{w1}, i.e. T_{14}. T_{14} and T are expressed as:

$$T_{14} = \frac{L_B + |v_{w2} - v_{w1}|T_{23}}{|v_{w4} - v_{w1}|} \quad (21)$$

$$T = T_{14} + T_{23} \quad (22)$$

The total numbers of ships affected by unclosed restricted segment N_B can be expressed as:

$$N_b = \rho_{B'_2}\left|v_{B'_2} - v_{w1}\right|T \quad (23)$$

5 The simulation of ship traffic flow characteristics based on Monte-Carlo

Ship traffic flow characteristic analysis is an important part of ship traffic flow simulation. Monte-Carlo method is commonly used in ship traffic flow simulation. It applies the random simulation technique (including stochastic simulation and statistical test) to analyze their probability distribution based on the historical data of the input variables, then randomly sample according to the probability distribution, and use the sampled-results of the input variables to simulate and solve the established mathematical model of the output variables. And after many simulations, the final simulation results are closer to the actual situation of ship traffic flow. According to the historical data of ship traffic flow in the middle reaches of the Yangtze River, SPSS (Statistical Product and Service Solutions) software was used in this paper to analyze the characteristics of ship traffic flow such as the laws of ship arrival, distribution of ship speed and ship types and so on; then Crystal Ball software was used in Monte Carlo method to construct the random numbers with the similar probability distributions of input variables, simulate the generation of ship traffic flow, and study the ship traffic flow in the closed and unclosed restricted channel segments.

5.1 Research on vessel traffic flow characteristics in the middle reaches of the Yangtze River

The middle reaches of the Yangtze River starts from Yichang, Hubei Province, and ends at the Hukou, Jiangxi Province, with a total length of 927 km. The most troublesome segment in the middle reaches of the Yangtze River is the Zhicheng-Chenglingji segment, also known as the Jingjiang

Table 1 Average monthly daily ship traffic flow rate of Jingzhou Yangtze River Bridge in 2013 (ves/day)

Month	1	2	3	4	5	6	7	8	9	10	11	12
Upstream traffic flow rate	84	35	70	78	101	88	63	92	92	72	95	77
Downstream traffic flow rate	103	39	76	101	133	95	92	109	96	88	119	92

segment, which is a "bottleneck" on the Yangtze's golden waterway. This paper selected the 2013 annual monitoring data of Jingzhou Yangtze River Highway Bridge located in the lower segment of Taipingkou waterway (the latest data cannot be obtained, so 2013 data was used for research).

5.1.1 Law of ship arrival

According to the monitoring data of Jingzhou Yangtze River Highway Bridge in 2013, the average monthly daily ship traffic flow rate is shown in Table 1.

According to season and month, the middle reaches of the Yangtze River can be divided into three periods: flood, moderate and dry periods. In general, the flood period is from May to October; the dry period from December to March of the following year; and the moderate period from April to November. As can be seen from Table 1, the ship traffic flow generally conforms to the variation of the river reach in the flood, moderate and dry periods, but this change is not very obvious because the overall ship traffic flow is not large.

The number of ships arriving in different time periods is observed continuously for 24 h, as shown in Table 2.

Table 2 Statistical mean of hourly ship traffic flow rate in a day (ves/h)

Time period/h	0 ~ 1	1 ~ 2	2 ~ 3	3 ~ 4	4 ~ 5	5 ~ 6	6 ~ 7	7 ~ 8	8 ~ 9	9 ~ 10	10 ~ 11	11 ~ 12
Upstream traffic flow rate	0	0	0	0	0	0	0	5	5	7	6	7
Downstream traffic flow rate	0	0	0	0	0	0	1	5	7	8	8	8
Time period/h	12 ~ 13	13 ~ 14	14 ~ 15	15 ~ 16	16 ~ 17	17 ~ 18	18 ~ 19	19 ~ 20	20 ~ 21	21 ~ 22	22 ~ 23	23 ~ 24
Upstream traffic flow rate	7	8	9	7	9	7	5	4	2	0	0	0
Downstream traffic flow rate	9	9	10	9	11	9	7	4	2	1	1	0

Table3 One-Sample Kolmogorov–Smirnov test of Normal distribution

Items		Upstream traffic flow rate	Downstream traffic flow rate	Upstream ship speed	Down-stream ship speed
N		24	24	15	15
Normal Parameters[a,b]	Mean	3.67	4.54	76.80	90.80
	Std. Deviation	3.485	4.107	16.537	22.625
Most Extreme Differences	Absolute	.270	.222	.135	.121
	Positive	.270	.222	.072	.095
	Negative	– .164	–.184	–.135	–.121
Kolmogorov–Smirnov Z		1.324	1.090	.524	.469
Asymp. Sig. (2-tailed)		.060	.186	.946	.980

[a]Test distribution is Normal

[b]Calculated from data

Table 4 One-Sample Kolmogorov–Smirnov test of Poisson distribution

Items		Upstream traffic flow rate	Downstream traffic flow rate	Upstream ship speed	Down-stream ship speed
N		24	24	15	15
Poisson parameter[a,b]	Mean	3.67	4.54	76.80	90.80
Most extreme differences	Absolute	.391	.358	.221	.203
	Positive	.391	.358	.148	.203
	Negative	–.254	–.285	– .221	– .179
Kolmogorov–Smirnov Z		1.916	1.752	.855	.786
Asymp. Sig. (2-tailed)		.001	.004	.458	.567

[a] Test distribution is poisson

[b] Calculated from data

The researches of the ship arrival law in some Chinese seaports indicate that the law generally obeys the Poisson distribution or Normal distribution. In order to further verify these results, SPSS software was used to fit the data in Table 2 to analyze the law of ship arrival in different time periods within a day, and carry out Kolmogorov–Smirnov test. The results are shown in Tables 3 and 4.

It can be seen from Tables 3 and 4 that the law of upstream and downstream ships arrival at different time periods within a day do not conform to the Poisson distribution characteristics, but all conform to the Normal distribution characteristics, and Sig. values are all greater than 0.05 (The Sig. value represents the test value of significant difference. Sig. > 0.05 means to accept the null hypothesis), indicating good fitting degree, so the law of ship arrival follow Normal distribution.

5.1.2 Ship speed distribution

Ship speed distribution refers to the distribution range and law of the speed of all ships in the water area. The speed distribution of ships generally obeys to Normal, Weibull or Lognormal distributions. The ship speed distribution characteristics in the middle reaches of the Yangtze River are shown in Table 5.

The data in Table 5 were fitted with SPSS software (Statistical Product and Service Solutions) to analyze the speed distribution of upstream and downstream ships, and conduct Kolmogorov–Smirnov test. The results are shown in Tables 3 and 4. Both speed distributions of upstream and downstream ships obey to Normal and Poisson distributions, and both Sig. values are greater than 0.05, indicating a good fitting degree. As the Sig. value of Kolmogorov–Smirnov test of Normal distribution is larger than that of Poisson distribution, it shows that the data are more consistent with Normal distribution. The mean speed of upstream ships is 7 kn and that of downstream ships is 8 kn.

5.1.3 Density distribution characteristics

The density distribution of ship traffic flow reflects the congestion degree of ship flow in the water area. The density distribution of ship traffic flow is affected by channel width, geographical factors, water level change, pilot quality and many other factors. The density and its distribution of ship traffic flow are different concepts. The density of ship traffic flow in a certain area is relatively high, but the ship traffic flow may not be blocked. On the contrary, blockage or collision accidents may occur in the water area where the density of ship traffic flow is not too high, which depends on whether the density distribution of ship traffic flow is reasonable. If most of the same numbers of ships in a certain area are concentrated in a local water area, the possibility of blockage accident is much greater than that of the evenly distributed number of ships. These characteristics cannot be described by statistical laws.

5.1.4 Distribution of ship types

According to the statistical analysis of the collected data, there are three main types of ships that pass the Jingzhou Yangtze River Highway Bridge: general cargo ships, dangerous goods ships and container ships. Among upstream ships, the proportions of these three types of ships are 78.01%, 11.77% and 10.21% respectively. In downstream ships, the proportions of that are 77.11%, 11.57% and 14.99% respectively. According to China's the Navigation Standard of Inland Waterway, small ships with a length of less than 90 m in the segment account for more than 90%.

5.2 Traffic flow simulation test

Crystal ball software was used to perform Monte Carlo simulation, the simulation assumptions are as follows:

(1) The arrival state of ships is the mutually independent random process and obeys Normal distribution;
(2) Ship speed obeys Normal distribution;
(3) In the peak period, the Maritime Department adopts one-way traffic for this segment (downstream ships are released);
(4) Irrespective of ship type;
(5) In the case of extreme low water level, ship overtaking is prohibited after the ship enters the restricted segment in order to ensure safety.
(6) Ship traffic flow meets Greenshields' linear model;
(7) The width of upstream segments *A*, restricted segment *B* and downstream segment *C* is the same;

Table 5 The speed distribution of upstream and downstream ships (ves)

Speed section / kn	0 ~ 1	1 ~ 2	2 ~ 3	3 ~ 4	4 ~ 5	5 ~ 6	6 ~ 7	7 ~ 8	8 ~ 9	9 ~ 10	10 ~ 11	11 ~ 12	12 ~ 13	13 ~ 14	14 ~ 15
Number of upstream ship	0	1	2	4	11	23	11	18	14	2	1	1	0	0	0
Number of downstream ship	0	1	2	4	11	8	12	12	20	13	7	8	6	3	2

(8) The psychology of the ship's pilot and maneuvering behavior of ships when they merge are not considered;
(9) Taking the Taipingkou channel as the research object, which is located in the Jingjiang channel segment of the middle reaches of the Yangtze River. It has always been the key navigation obstacle, namely the segment *B*, whose with length L_B is 17.5 km. Small ships with the length of less than 90 m in the segment account for more than 90%. The distribution of ship types is not considered here, and the representative ship type CJB(2004)H1000-I in the middle reaches of the Yangtze River is taken as the research object.

5.2.1 Parameter settings

The main technical indicators of the ship type CJB(2004) H1000-I are 1000 tons (deadweight), 65.5 m long, 10.8 m wide, and v_f is 10 kn. According to the calculating results, the blocking density $\rho_j = 1000/((1+\beta)\ L_0)$, L_0 is the ship length; β is the ship spacing coefficient, generally $\beta = 0.5$. According to Eqs. (5–7), then the $\rho_j = 7.84$ ves/km; $\rho_m = \frac{1}{2}\rho_j = 3.92$ ves/km; $v_m = \frac{1}{2}v_f = 5$ kn. To unity the unit, the unit kn should be converted to km/h (1kn = 1.852 km/h). The simulated object is the ship traffic flow in the continuous segments *A-B-C* and the restricted segment *B*. For this traffic process, there are many parameters that will affect the congestion state of the segments. In the simulation test, five parameters are considered as input variables such as the ship traffic flow rate and average speed of upstream segment *A* and downstream segment *C*, and the difference of traffic flow rate between inflowed from segment *D* and outflowed from segment *B* (In the simulation test of closed restricted segment, the first four parameters are selected; and in that of unclosed restricted segment, five parameters are selected). In Crystal Ball software, these parameters are set as Assumption cells. The two parameters, the dissipation time of queuing and the total number of ships affected, are taken as the output variables and set as forecast cells, as shown in Table 6. Monte Carlo method was conducted for the dissipation time of queuing and the total number of ships affected in the closed and unclosed restricted segments respectively, and the simulating times were 1000. The simulation data were summarized, histograms were drawn, and the 10%, 90%, mean and median data of the statistical data were displayed. Finally, the sensitivity analysis table was generated.

5.2.2 Simulation test of the closed restricted segment

After 1000 times of simulations, the data results of 901 times are shown. Considering the randomness of the test results, these errors are deemed to be reasonable.

Table 6 Parameter settings

Parameters of the nature	Parameter name	Symbol	Unit	Input
Constant value	Length of segment *B*	L_B	km	17.50
	Length of segment B_1	L_{B_1}	km	10
	Length of segment B_2	L_{B_2}	km	7.5
	Free speed of ship	v_f	km/h	18.52
	Optimum speed of ship	v_m	km/h	9.26
	Blocking density	ρ_j	ves/km	7.84
	Optimum density	ρ_m	ves/km	3.92
	Maximum traffic flow rate	q_m	ves	36.3
	Ship traffic flow rate of segment *B*	q_B	ves/h	21.80
	Average speed of ship traffic flow of segment *B*	v_B	km/h	5.56
	Density of ship traffic flow of segment *B*	ρ_B	ves/km	3.92
Assumption cells	Ship traffic flow rate of segment *A*	q_A	ves/h	18
	Ship traffic flow rate of segment *C*	q_C	ves/h	18
	Average speed of ship traffic flow of segment *A*	v_A	km/h	14.82
	Average speed of ship traffic flow of segment *C*	v_C	km/h	14.82
	The difference of traffic flow rate between inflowed from segment *D* and outflowed from segment *B*	Δq_D	ves/h	8
Forecast cells	The dissipation time	T	h	
	The total number of ships affected	N_b	ves	

*q_A, q_C, v_A, v_C, Δq_D are mean values, and obey Normal distribution

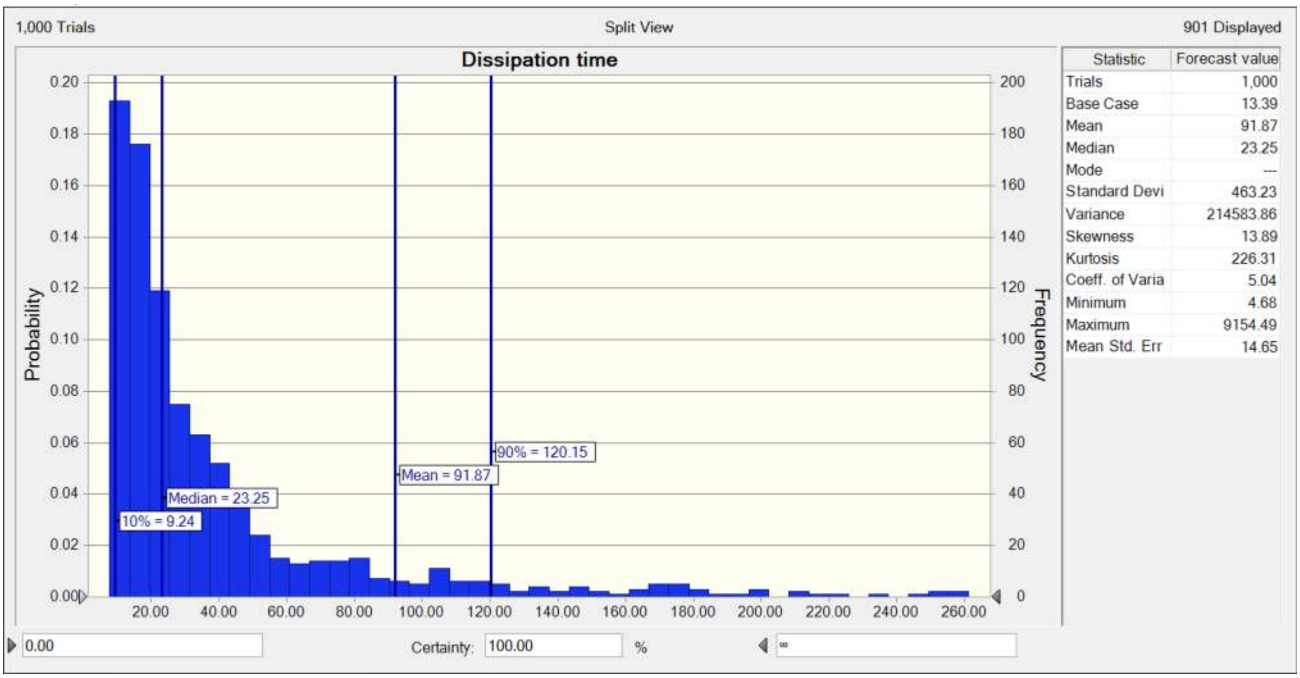

Fig. 8 Simulation results of dissipation time

Table 7 Sensitivity analysis of dissipation time

Assumption cells	Contribution to variance (%)
Ship traffic flow rate of segment *A*	– 37.6
Ship traffic flow rate of segment *C*	– 31.5
Average speed of ship traffic flow of segment *A*	10.9
Average speed of ship traffic flow of segment *C*	20.0

The simulation results and sensitivity analysis of the dissipation time are shown in Fig. 8 and Table 7 separately.

As shown in Fig. 8 and Table 7, the mean dissipation time is 91.87 h, the median is 23.25 h, and the 90% probability of dissipation time is within 120.15 h. According to the sensitivity analysis, the ship traffic flow rate of segments *A* and *C* are negatively correlated with the dissipation time. The average speed of ship traffic flow of segments *A* and *C* are positively correlated with the dissipation time. A positive correlation coefficient implies that an increase in the hypothesis will result in an increase in the dissipation time, while a negative correlation coefficient implies the opposite.

The simulation results and sensitivity analysis of the number of ships affected are shown in Fig. 9 and Table 8 separately.

As shown in Fig. 9 and Table 8, the mean of the total number of ships affected is 1485.02 ves, the median is 383.64 ves, and the 90% probability of the total number of ships affected is within 2055.93 ves. According to sensitivity analysis, the ship traffic flow rate and the average speed of ship traffic flow of segment *A*, and the average speed of ship traffic flow of segment *C* are positively correlated with the total number of ships affected, and the variance contribution of ship traffic flow rate of segment *A* is as high as 79.4%. But the correlation between ship traffic flow rate in segment *C* and the total number of ships affected is negative.

The results show that the larger the ship traffic flow rate of segments *A* and *C*, the shorter the dissipation time. The larger the average speed of ship traffic flow of segments *A* and *C*, the longer the dissipation time. Ship traffic flow rate of segment *A* is the key factor of the total number of ships affected.

5.2.3 Simulation test of the unclosed restricted segment

(1) $T_{23} > T_{31}$

When $T_{23} > T_{31}$, the simulation results and sensitivity analysis of the dissipation time are shown in Fig. 10 and Table 9 separately.

As shown in Fig. 10 and Table 9, the mean dissipation time is 2.41 h, the median is 2.09 h, and the 90% probability of dissipation time is within 3.23 h. According to the sensitivity analysis, the ship traffic flow rate of segment

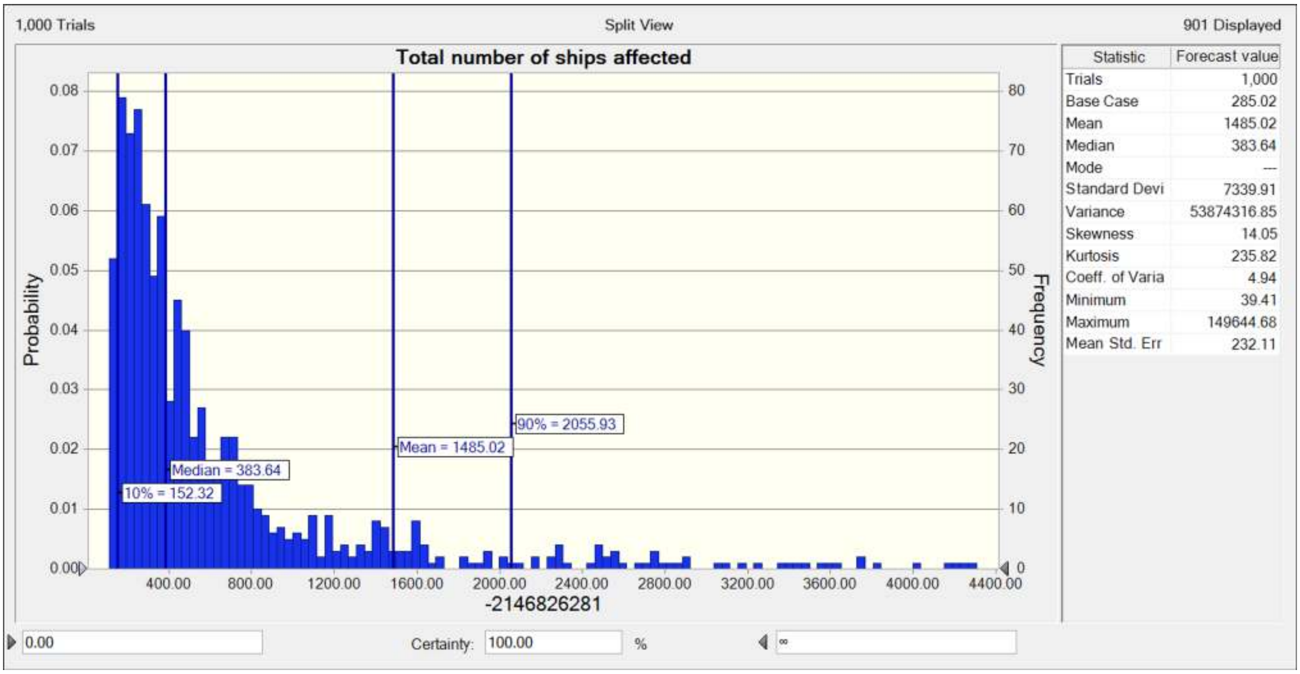

Fig. 9 Simulation results of the number of ships affected

Table 8 Sensitivity analysis of the total number of ships affected

Assumption cells	Contribution to variance (%)
Ship traffic flow rate of segment *A*	79.4
Ship traffic flow rate of segment *C*	– 5.7
Average speed of ship traffic flow of segment *A*	8.8
Average speed of ship traffic flow of segment C	6.1

C is positively correlated with the dissipation time, and the variance contribution is as high as 90.1%. The average speed of ship traffic flow of segments *A* and the difference of traffic flow rate between inflowed from segment *D* and outflowed from segment *B* (Δq_D) are negatively correlated with dissipation time, where the variance contribution of Δq_D is 9.4%.

When $T_{23} > T_{31}$, the simulation result and sensitivity analysis of the number of ships affected are shown in Fig. 11 and Table 10 separately.

As shown in Fig. 11 and Table 10, the mean of the total number of ships affected is 64.61 ves, the median is 54.89 ves, and the 90% probability of the total number of ships affected is within 102.12 ves. According to sensitivity analysis, the ship traffic flow rate of segment *A* is positively correlated with the total number of ships affected, and the variance contribution is as high as 99.4%. The average speed of ship traffic flow of segment *A* and *C* are negatively correlated with the total number of affected ships, with the total variance contribution of 0.5%.

The results show that the ship traffic flow rate of downstream segment *C* and Δq_D will greatly affect the dissipation time, while the ship traffic flow rate of upstream segment *A* is the decisive factor of the total number of affected ships.

(2) $T_{23} < T_{31}$

When $T_{23} < T_{31}$, the simulation results and sensitivity analysis of the dissipation time are shown in Fig. 12 and Table 11 separately.

As shown in Fig. 12 and Table 11, the mean dissipation time is 117.21 h, the median is 39.23 h, and the 90% probability of dissipation time is within 189.50 h. According to the sensitivity analysis, the ship traffic flow rate and average speed of segment *C* are negatively correlated with the dissipation time, and the sum of variance contribution is 72.3%. The ship traffic flow rate and average speed of segment *A*, and Δq_D are positively correlated with dissipation time, and the sum of variance contribution is 27.7%.

When $T_{23} < T_{31}$, the simulation results and sensitivity analysis of the number of ships affected are shown in Fig. 13 and Table 12 separately.

As shown in Fig. 13 and Table 12, the mean of the total number of ships affected is 2223.88 ves, the median is 745.15 ves, and the 90% probability of the total number of ships affected is within 3725.99 ves. According to the

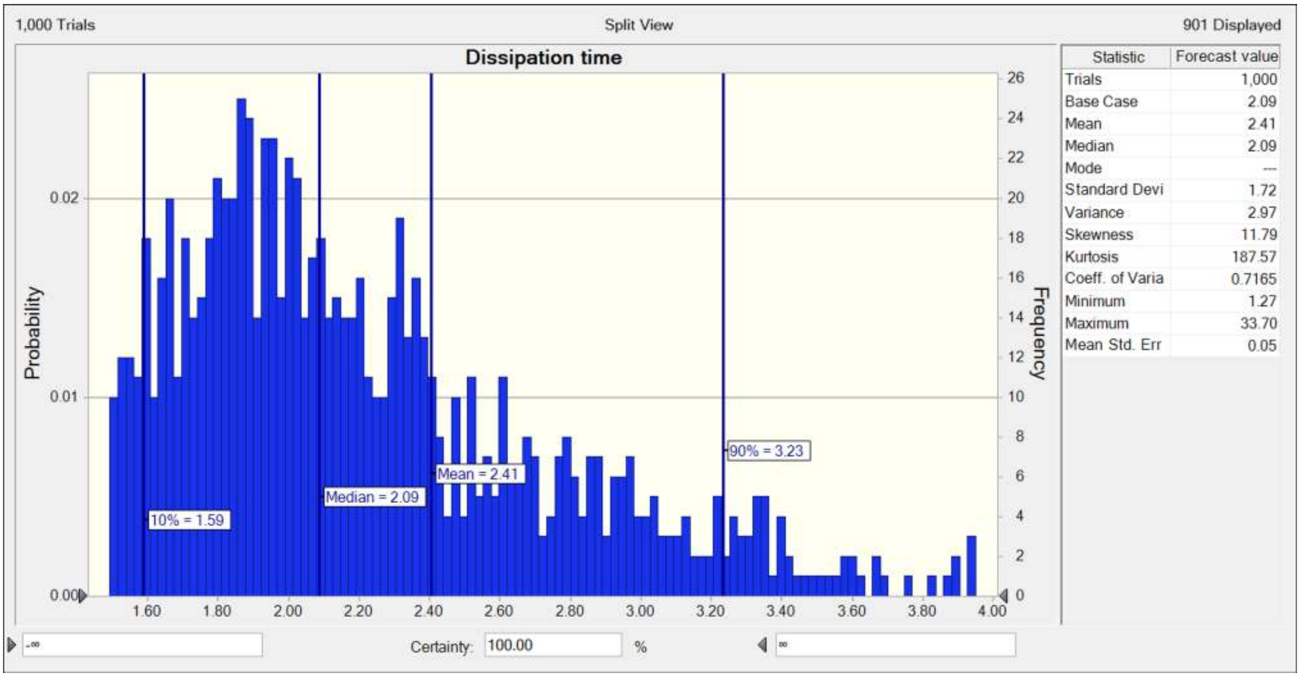

Fig. 10 Simulation results of dissipation time ($T_{23} > T_{31}$)

Table 9 Sensitivity analysis of dissipation time ($T_{23} > T_{31}$)

Assumption cells	Contribution to variance (%)
Ship traffic flow rate of segment *A*	0.2
Ship traffic flow rate of segment *C*	90.1
Average speed of ship traffic flow of segment *A*	– 0.1
Average speed of ship traffic flow of segment *C*	0.2
The difference of traffic flow rate between inflowed from segment *D* and outflowed from segment *B* (Δq_D)	– 9.4

sensitivity analysis, the ship traffic flow rate of segment *A* and Δq_D are positively correlated with the total number of affected ships, in which the variance contribution of ship traffic flow rate of segment *A* is as high as 86.8%. The average speed of ship traffic flow of segments *A* and *C*, and the ship traffic flow rate of segment *C* are negatively correlated with the total number of affected ships, with the total variance contribution of 8.6%.

The results show that the ship traffic flow rate of downstream segment *C* and Δq_D will greatly affect the dissipation time, while the ship traffic flow rate of upstream

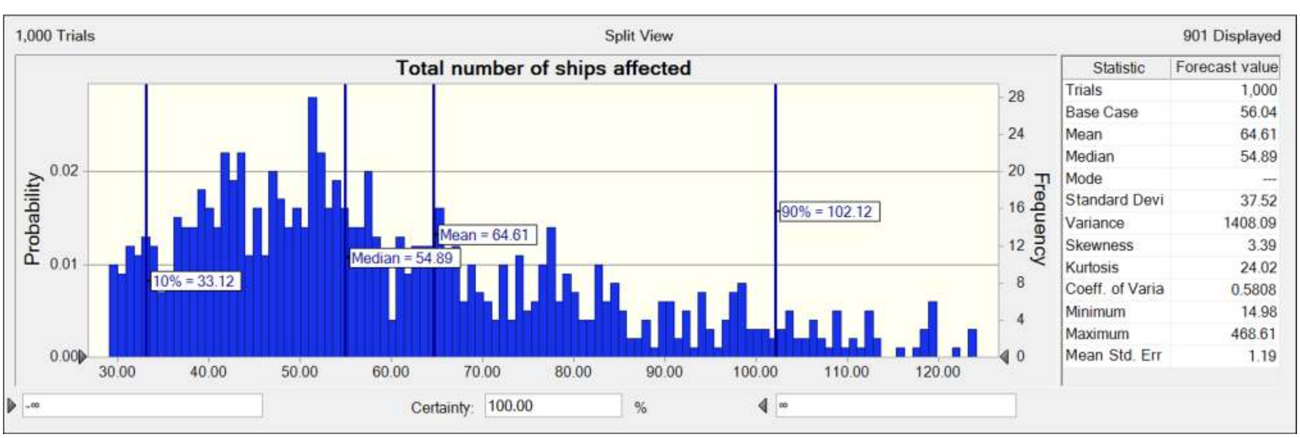

Fig. 11 Simulation result of the number of ships affected ($T_{23} > T_{31}$)

Table 10 Sensitivity analysis of the total number of ships affected ($T_{23} > T_{31}$)

Assumption cells	Contribution to variance (%)
Ship traffic flow rate of segment *A*	99.4
Ship traffic flow rate of segment *C*	0
Average speed of ship traffic flow of segment *A*	− 0.4
Average speed of ship traffic flow of segment *C*	− 0.1
The difference of traffic flow rate between inflowed from segment *D* and outflowed from segment *B* (Δq_D)	0.1

Table 11 Sensitivity analysis of dissipation time ($T_{23} < T_{31}$)

Assumption cells	Contribution to variance (%)
Ship traffic flow rate of segment *A*	7.1
Ship traffic flow rate of segment *C*	− 71.7
Average speed of ship traffic flow of segment *A*	0.2
Average speed of ship traffic flow of segment *C*	− 0.6
The difference of traffic flow rate between inflowed from segment *D* and outflowed from segment *B* (Δq_D)	20.4

segment *A* is the key factor to determine the total number of affected ships.

6 Summary of simulation tests

The simulation results of ship traffic flow of closed and unclosed restricted segment show that the total number of ships affected is highly positively correlated with the ship traffic flow rate of upstream segment. During the peak period of the ship traffic flow, the total number of ships affected will enhance as the traffic flow rate of upstream segment increases. Dissipation time is different between closed and unclosed restricted segments. In closed restricted segment, dissipation time is mainly related to ship traffic flow rate of segment *A* and *C*, while in unclosed restricted segment, dissipation time is mainly related to ship traffic flow rate of segment *C* and Δq_D. In closed restricted segment, the total number of ships affected is mainly related to ship traffic flow rate of segment *A*. And in unclosed restricted channel segment, the dissipation time and the total number of ships affected are also determined by the meeting time of the traffic waves in addition to the ship traffic flow rate of segments. The values of dissipation time and the total number of ships affected at $T_{23} > T_{31}$ are significantly smaller than those at $T_{23} < T_{31}$.

7 Discussion

7.1 Main research results and significance

(1) The formation mechanism of multiple traffic waves (≥ 3) and the correlation between traffic wave speed

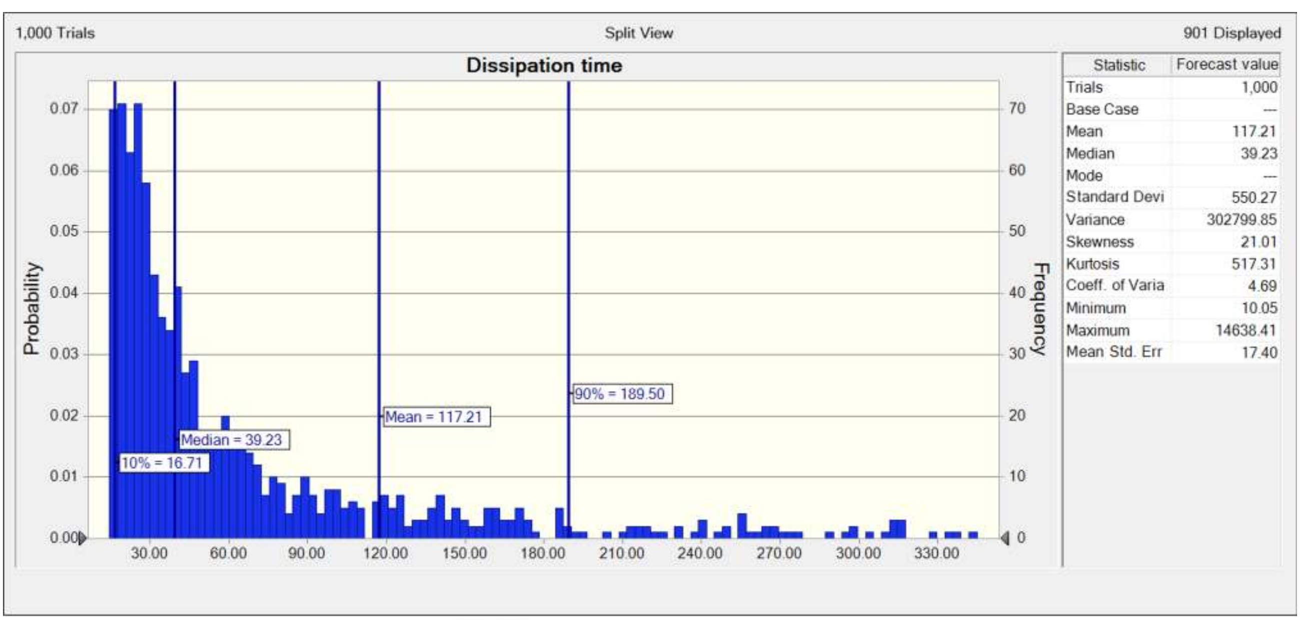

Fig. 12 Simulation results of dissipation time ($T_{23} < T_{31}$)

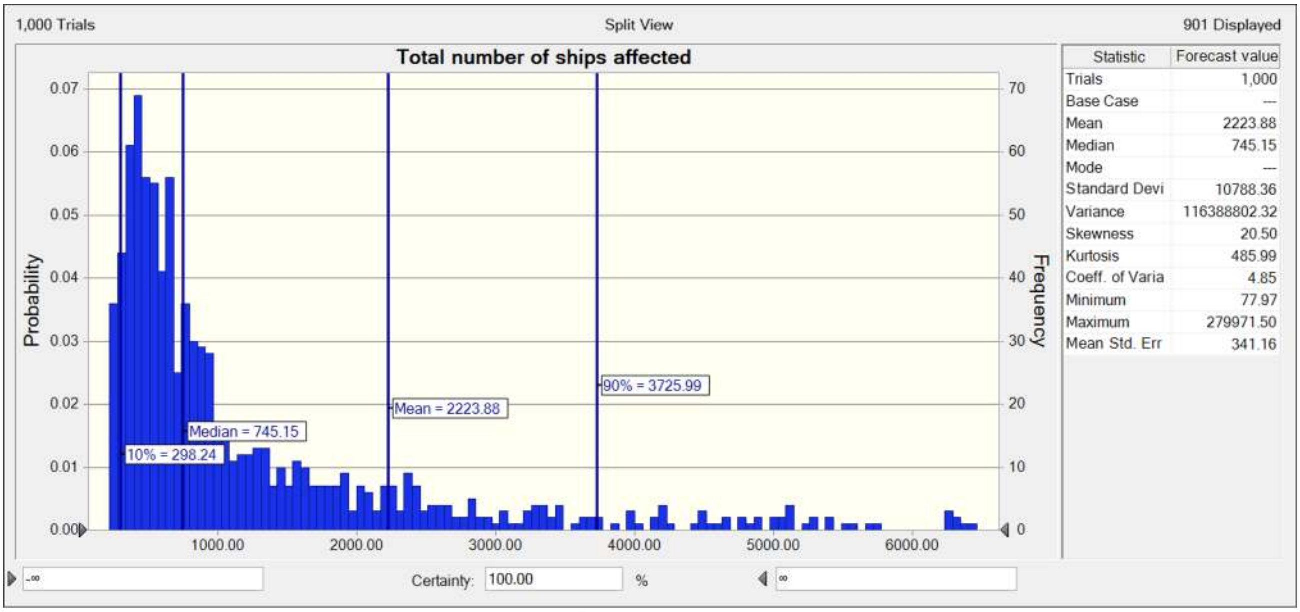

Fig. 13 Simulation results of the number of ships affected ($T_{23} < T_{31}$)

Table 12 Sensitivity analysis of the total number of ships affected ($T_{23} < T_{31}$)

Assumption cells	Contribution to variance (%)
Ship traffic flow rate of segment *A*	86.8
Ship traffic flow rate of segment *C*	− 8.4
Average speed of ship traffic flow of segment *A*	− 0.1
Average speed of ship traffic flow of segment *C*	− 0.1
The difference of traffic flow rate between inflowed from segment *D* and outflowed from segment *B* (Δq_D)	4.6

and ship traffic flow rate, ship speed and density of each segment are given in the unclosed restricted segment (i.e., the restricted segment with tributaries). The influence of speed and direction of traffic wave on the ship traffic flow is more complex. Under certain conditions, the ship on the voyage will produce multiple gathering and dissipating waves at the same time. When two traffic waves of the same nature meet, a new traffic wave will be generated. When two traffic waves of different nature meet, the queued ships will dissipate and the channel blockage will be relieved.

(2) The traffic condition of the unclosed restricted segment is more complicated than that of the closed restricted segment. Due to the inflow of traffic flow rate of tributary, the direction of the traffic wave speed will have a great impact on the dissipation time of queued ships and the total number of affected ships. The relevant parameter expressions in different situations are given.

The research results can enrich the theoretical study of inland ship traffic flow to a certain extent, and provide theoretical support for making navigation control strategy scientifically. The research has a certain theoretical significance and practical application value for reducing the influence of the extreme hydrological events in the middle reaches of Yangtze River on the shipping, improving navigation efficiency and competitiveness of shipping, and developing Yangtze River Belt.

8 Research features

Based on the ship traffic flow theory and the Greenshields linear model, this study focuses on the formation of multiple traffic waves (≥ 3) in the unclosed restricted segment of inland river under extreme water level conditions, as well as the influence laws of the corresponding gathering wave and dissipating wave on ship traffic flow, and gives the relevant parameter expressions. This research results have certain characteristics, which is different from the related research in China and abroad. Many scholars study traffic flow theory in normal water level, including the passing capacity or passing efficiency of ships in inland channel segment, characteristics of traffic flow, traffic congestion state, traffic flow rate, density and speed, and related simulation tests, as well as gathering and dissipation process of ship traffic flow based on traffic wave theory, etc.

From the perspective of domestic and foreign researches, there are few studies on the impact of extreme water level changes on the ship traffic flow of inland river, especially the formation of multiple traffic waves and their effects on both gathering and dissipation waves of unclosed and unclosed restricted segments.

8.1 Existing deficiencies

The ship traffic flow discussed in this paper is only limited to the closed and unclosed restricted segments with one-way traffic in peak periods, as well as the meeting situation of two traffic waves. There are still many complex issues that have not been covered and need to be further studied in the future. For example, the unsteady ship traffic flow, the two-way ship traffic flow, the ship traffic flow with different ship types and crossing the main segment, the influence of the location of the tributary on the ship traffic flow of the main segment, and the situation where multiple tributaries merge into restricted segment, etc.

9 Conclusions

This paper focuses on the study of the internal relationship between ship traffic congestion and traffic waves in the closed and unclosed restricted segments and the following conclusions are drawn:

(1) The expressions of traffic wave speed and direction, the dissipation time and the total number of ships affected were given, which provides theoretical support for the simulation calculation of ship traffic flow in such channel segment.
(2) The dissipation time of the queued ship of closed restricted segment is mainly related to the ship traffic flow rate of segments *A* and *C*, and the total number of ships affected is highly positively correlated with the ship traffic flow of the upstream segment *A*.
(3) The dissipation time of the queued ship of unclosed restricted segment is mainly related to the ship traffic flow rate of segment *C* and the difference of traffic flow rate between inflowed from segment *D* and outflowed from segment *B*. The total number of ships affected is positively correlated with the ship traffic flow rate of the upstream segment *A*, and when $T_{23} > T_{31}$, both the dissipation time and the total number of ships affected are significantly less than those when $T_{23} < T_{31}$.
(4) The interaction and influence laws between multiple traffic waves were given, as well as the process of the two traffic waves meeting and the formation rule of the new traffic wave, including the speed and direction of the new traffic wave and its influence on the ship traffic flow.

The ship traffic flow discussed in this paper is only limited to closed and unclosed restricted segments of one-way traffic in peak periods, and many problems have not been dealt with yet, which are worthy of further study, are shown in 6.2.

Acknowledgements This research has been supported in part by China Scholarship Council under Grant 201808360307, and in part by Humanities and Social Sciences Project of Department of Education of Jiangxi Province under Grant JC17234, and Social Science Planning Project of Jiangxi Province under Grant 15YJ04.

Declarations

Conflict of interest On behalf of all authors, the corresponding author states that there is no conflict of interest.

References

1. Wang D (2002) Traffic flow theory. Beijing, China
2. Ren F (2008) Traffic engineering. Beijing, China
3. Wu Z (1993) Marine traffic engineering. Dalian, China
4. Liu Y (2014) Study on vessel flow organization on extreme water levels in the middle Yangtze River. Ph.D. Dissertation, Wuhan Univ. of Technol
5. Lu S, Liu Y (2017) Impact of extreme water levels on characteristics of vessel traffic flow in the middle reaches of Yangtze River. J Chongqing Jiaotong Univ (Natural Sci) 36(3):103–107 https://doi.org/10.3969/j.issn.1674-0696.2017.03.17
6. Liu Z, Liu J, Zhou F, Guoi W (2014) Behavior characteristics of vessel traffic flow and traffic organization. J Dalian Marit 40(2):88–101
7. Liao P (2009) Temporal and spatial distribution of traffic flow in inland waterways. Hydro-Sci Eng 2:33–38. https://doi.org/10.3969/j.issn.1009-640X.2009.02.006

8. Elloumi SZ, Roy V, Marmorat JP et al (2014) Securing harbor by combining probabilistic approach with event-based approach. Appl Ocean Res 47:98–109
9. Treiber M, Kesting A (2013) Traffic flow dynamics: data, models and simulation. Springer, Heidelberg, New York, Dordrecht, London
10. Kujala P, Hanninen M, Arola T et al (2009) Analysis of the marine traffic safety in the Gulf of Finland. Reliab Eng Syst Saf 94(9):1349–1357. https://doi.org/10.1016/j.ress.2009.02.028
11. Liu Z (2017) Study on characteristics and evolution models of vessel traffic flow for complex navigation system. Ph.D. Dissertation, Wuhan Univ. of Technol.
12. Dong Y, Jiang Y, He L (2007) Calculation method of inland waterways throughput capacity. Port Waterway Eng 1:59–65. https://doi.org/10.3969/j.issn.1002-4972.2007.01.015
13. Zhang W, Liu J, Sun H, Liu H, Chu M (2016) Research on channel transit capacity in Yangtze River deepwater channel. China Harb Eng 36(2):5–10. https://doi.org/10.7640/zggwjs201602002
14. Yang X, Yang X, Wang Z, Liu K, Li J (2019) Marine traffic simulation of congestion in restricted waterway with Mont Carlo Method. Navi China 36(2):40–44. https://doi.org/10.3969/j.issn.1000-4653.2016.02.010
15. Elefteriadou L (2014) An introduction to traffic flow theory. Springer, New York
16. Ma J (2004) Fundamentals of traffic flow theory. People's Public Security University of China Press, Beijing
17. Ali A, Andallah LS (2016) Inflow outflow effect and shock wave analysis in a traffic flow simulation. Am J Comput Math 6:55–65. https://doi.org/10.4236/ajcm.2016.62007
18. Rakha H, Crowther B (2002) Comparison of greenshields, pipes, and van aerde car-following and traffic stream models. Transp Res Rec 1:248–262. https://doi.org/10.3141/1802-284
19. Gaus A, Muhammad TYS, Ambo USH, Liska N (2021) Mathematical model of traffic speed and capacity in the archipelago base. In: IOP Conference Series: Materials Science and Engineering 1125(1). https://doi.org/10.1088/1757-899X/1125/1/012023
20. Zhang P, Liu Y, Liu H (2014) Analysis of inland ship traffic flow organizational characteristics based on traffic wave theory. Appl Mech Mater 644–650:1883–1886
21. Bai X, Xiao Y, Sun Y, Zhen J (2014) Traffic efficiency of north deep water channel based on traffic wave theory. Navig China 37(1):61–65. https://doi.org/10.3969/j.issn.1000-4653.2014.01.014
22. Zeng S (2019) Analysis of transport efficiency in Wusong Warning Zone based on traffic wave theory. J Qingdao Ocean Shipp Mar Coll 40(2):49–53. https://doi.org/10.3969/j.issn.2095-3747.2019.02.010
23. Feng H, Xiao Y, Kong F, Yang X (2013) Cellular automaton model for partial reduction lane based on ship automatic identification system. J Shanghai Marit Univ 34(3):22–31. https://doi.org/10.3969/j.issn.1672-9498.2013.03.005
24. Feng H, Kong F, Xiao Y, Yang X (2014) AIS-based cellular automaton modeling of waterway moving bottleneck. J Wuhan Univ Technol 38(2):324–328. https://doi.org/10.3969/j.issn.1000-4653.2014.01.019
25. Wang Z, Liu K, Yang X, Yang F, Yang X (2018) Probability of ship speed reducing in one-way channel. Navig China 41(4):42–46. https://doi.org/10.3969/j.issn.1000-4653.2018.04.009
26. Cai X, Liu K, Yang X, Tian W, Liu J (2012) Traffic flow simulation in inland waterway intersection area. J. Dalian Marit Univ 38(2):19–21. https://doi.org/10.16411/j.cnki.issn1006-7736.2012.02.016
27. Zhou H (2014) Vessel traffic statistics and simulation research for waterway in bridge area of Yangtze River. Master thesis, Dalian Maritime Univ
28. Wang W, Peng Y, Tian Q et al (2017) Key influencing factors on improving the waterway through capacity of coastal ports. Ocean Eng 137:382–393. https://doi.org/10.1016/j.oceaneng.2017.04.013
29. Asperen EV (2003) Modeling ship arrivals in ports. In: Proceedings of the 2003 Winter Simulation Conference, 2003
30. Ercan K, Ersan B, Emrullah D et al (2003) Simulation of marine traffic in Istanbul strait. Simul Model Pract Theory 11(7):597–608. https://doi.org/10.1016/j.simpat.2003.10.001
31. Kawamura K, Hashimoto H, Matsuda A et al. (2016) SPH simulation of ship behaviour in severe water-shipping situations. In: 1st International Meeting on Propeller Noise and Vibration
32. Qi L, Zheng Z, Gang L (2017) A cellular automaton model for ship traffic flow in waterways. Phys A 471:705–717. https://doi.org/10.1016/j.physa.2016.12.028
33. Qi L, Zheng Z, Gang L (2017) Marine traffic model based on cellular automaton: considering the change of the ship's velocity under the influence of the weather and sea. Phys A 483:480–494. https://doi.org/10.1016/j.physa.2017.04.125
34. Feng H (2013) Cellular automata ship traffic flow model considering integrated bridge system. Sci Technol 6(6):121–132. https://doi.org/10.14257/ijunesst.2013.6.6.12